Steady Laminar Round Jets of a Viscous Liquid Falling Vertically in the Atmosphere

The shape of a laminar, liquid jet emerging from a round vertical tube into the atmosphere and the total axial force exerted on the liquid filament at the tube exit were investigated experimentally over a wide range of flow conditions. An integral invariant of the exact solution was used to check consistency between the two kinds of data. A new equation to predict the jet shape agreed moderately well with the present experimental data as well as with various previous results. The key idea of the present work is that exact knowledge of the total axial force will be very useful to predict reasonably the jet shape at a given flow condition by means of a simplified approach or to check theoretical or empirical results on free falling jets.

K. Adachi
K. Tagashira
Y. Banba
H. Tatsumi
H. Machida
N. Yoshioka
Department of Chemical Engineering
Kyoto University
Kyoto, 606, Japan

Introduction

The study of vertical liquid jets is of interest in connection with spinning and rheological measurement of extension characteristics. It is also important in curtain coating and film casting because certain results for round vertical jets are expected to be useful even for plane jets, as was suggested by Clarke (1968) and Cruickshank (1984). Steady, laminar, round jets of viscous liquids, issuing from a vertical tube nozzle into the air and falling freely under gravity, have been investigated by many researchers (Trouton, 1906; Duda and Vrentas, 1967; Shirazi, 1978; Petrie, 1979; Dutta and Ryan, 1982; Joseph et al., 1983; Trang and Yeow, 1986; Mendizabal et al., 1987). Today, proper numerical simulations by finite-element methods seem to yield moderate predictions of the jet shapes at arbitrary flow conditions (Georgiou et al., 1988).

Existing measured or calculated results of jet shapes are often inconvenient to use for engineering purposes because of their numerical expressions. It is important for engineering scientists to have a simple analytical equation predicting the jet shapes at arbitrary flow conditions, when they utilize those results to solve more complicated flow problems in industries. The usefulness of such an equation has been shown by Adachi et al. (1988) in studying the V-shape of a steady, vertical, plane liquid jet with the two free side edges.

In previous investigations of vertical liquid jets is there have been many reports for jet shapes but none for forces exerted on the liquid filament of a free falling jet. However, it is clear that not only the jet shape but also the total axial force at a nozzle exit is important to understand the fluid mechanics of a vertical liquid jet, as the flow pattern and the drag force are both important for the fluid mechanics of flow past a submerged body. As explained in the next section, the total axial force equals exactly the constant value that is taken at a given flow condition by a certain integral invariant to the exact solution of the relevant flow problem. This relation can be used to test the validity of measured and calculated results of jet shapes and moreover to check consistency between the jet shape and the total axial force determined at the same flow condition.

There are three purposes in the present paper. The first, and most important, is to report the data of total axial forces measured over a wide range of flow conditions under a significant effect of gravity for free falling jets. Regrettably there is nothing available to compare with those data.

The second purpose is to present the data of jet shapes, which were measured in pairs together with total axial forces at the same flow conditions, that is, which are consistent with those of total axial forces.

The last purpose is to test a simple analytical equation of the jet shape in comparison with present experimental data.

Predictions of the simple equation are compared also with computational results of Duda and Vrentas (1967) and Shirazi (1978) and experimental results of Trang and Yeow (1986). Comparisons with computational results of Dutta and Ryan (1982) and Georgiou et al. (1988) are not made. Those of Dutta and Ryan are incorrect, as was shown by Adachi and Yoshioka (1984). Those of Georgiou et al. (1988) are expected to agree with predictions of the relevant equation because those authors

Correspondence concerning this paper should be addressed to K. Adachi.

have shown a good agreement between their predictions and present experimental data in two cases. The equation tested in the present paper will be found useful over such a wide range of flow conditions that $Re < 0(10^2)$, $Fr < 0(1)$, and $N_j > 0(1)$.

The relevant analytical equation of the jet shape is derived from a one-dimensional jet flow model on the assumption of flat profiles of velocity and pressure over the horizontal cross section. The following type of equation has been proposed by several researchers:

$$\frac{1}{Fr}\frac{z}{R} = \left(\frac{R}{a}\right)^4 - \delta_i + \frac{\beta}{We}\left(\frac{R}{a} - 1\right) \tag{1}$$

where

$$\begin{aligned} \delta_i = 1 \quad \beta &= 0 \text{ (Scriven and Pigford, 1959)} \\ = 1 \quad &= 8 \text{ (Kurabayashi, 1959)} \\ = 16/9 \quad &= 0 \text{ (Lienhard, 1968)} \\ = 1 \quad &= 4 \text{ (Anno, 1977)} \end{aligned}$$

However such equations are useless in a range of low Reynolds numbers. An equation that is valid over a wide range of Reynolds numbers has been derived by Clarke (1968):

$$U(X) = 1/2^{1/3}\{[A_i'(r)/A_i(r)]^2 - r\};\ r = (X + k)/2^{1/3} \tag{2}$$

where A_i is the Airy function, the prime associated with it denotes differentiation with respect to r, k is a constant, and

$$U = (u/\bar{u}_0)\,(ReFr/3)^{1/3},\ X = (z/R)\,(ReFr/72)^{1/3} \tag{3}$$

However this will not be useful for engineering purposes until the way in which to specify a reasonable value of the adjustable parameter k for an arbitrary flow condition is given. A new equation, which is proposed here to test, is produced by a simple addition of two terms valid at low and high Reynolds numbers:

$$\frac{1}{Fr}\frac{z}{R} = \left(\frac{R}{a}\right)^4 - \delta_i + \left\{\frac{2}{We} + \left[\left(\frac{2}{We}\right)^2 + \frac{24}{Re \cdot Fr}\right]^{1/2}\right\}\left(\frac{R}{a} - \delta_v\right) \tag{4}$$

Here the two adjustable parameter δ_i and δ_v are constants whose values are given in the appendix.

Theoretical Background

Macroscopic momentum balance

For a steadily falling round jet, as seen in Figure 1, the macroscopic balance equation of axial momentum can be expressed as

$$F_0 = F(z) + W(z) \tag{5}$$

where

$$F(z) = 2\pi\sigma a/(1 + \dot{a}^2)^{1/2} + 2\pi\int_0^a (\tau_{zz} - p + p_a - \rho u^2)\, r dr \tag{6}$$

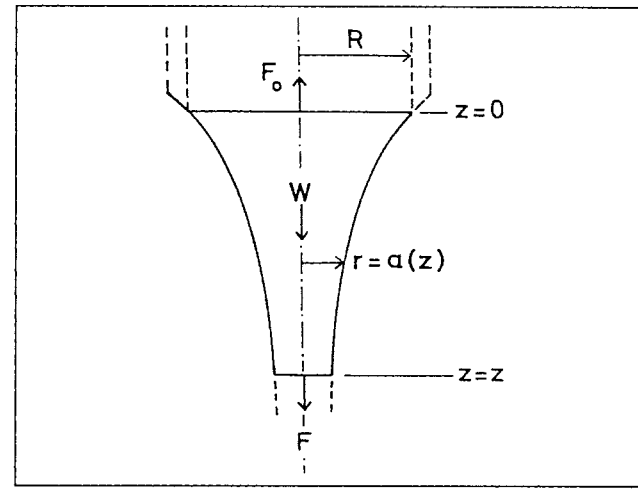

Figure 1. Force balance for a suspending jet filament.

$$W(z) = \pi\rho g\int_0^z a^2\, dz \tag{7}$$

The term F_0, which is defined by $F(0)$, is the total axial force exerted on the upper end of the suspending filament of an imaginarily semiinfinite length, $F(z)$ is the total axial force acting on the filament at the position of interest z, and $W(z)$ is the weight of the suspending filament from its upper end ($z = 0$) to z. Equation 5 expresses the balance of these three forces, and it indicates that both $F(z)$ and $W(z)$ vary with z, but their sum, $F(z) + W(z)$, is an integral invariant that is kept constant along the vertical axis of z, as pointed out by Joseph (1980). Moreover, Eq. 5 requires that the constant value be equal to F_0. These two points can be used to test the appropriateness of a jet shape function $a(z)$. Equation 6 represents that the total axial force consists of the following four forces: surface tension, viscous drag, static pressure, and inertia force.

For a Newtonian fluid the viscous drag term vanishes at the plane of the nozzle exit, so that F_0 is given by

$$F_0 \equiv F(0) = 2\pi R\sigma/(1 + \dot{a}_0^2)^{1/2} + 2\pi\int_0^R (p_a - p_0 - \rho u_0^2)\, r dr \tag{8}$$

When the jet shape function becomes known by experiments, $W(z)$ can be estimated through Eq. 7, but $F(z)$ cannot be estimated through Eq. 6 because the integrant is still unknown. Far downstream from the nozzle exit, it can be assumed that the profiles of axial velocity and static pressure are flat over the horizontal cross section of a vertical jet, and that $|\dot{a}| \ll 1$. Then the following approximate equation can be derived in a way similar to that in the case of a vertical plane jet (Adachi, 1987):

$$F(z) \simeq \pi\sigma a + \pi a^2\,(3\mu d\bar{u}/dz - \rho\bar{u}^2) \tag{9}$$

Experimental Method

Only the steady vertical jet without air drag was investigated. The main part of the jet was neither so thin nor of such high velocity that air drag became significant. The main part was not influenced by the oscillation of the jet tail because the tail was

much thinner than the main part. Thus the measured force F_0 did not change even if the vertical jet flow was interrupted by a horizontal plate at a distance far downstream from the nozzle exit.

The central part of the present work was to measure the jet radius $a(z)$ and the total axial force F_0 as accurately as possible. Jet radius data obtained from photographs are usually of much lower accuracy than axial force data measured directly with an electric weighing device. Over the total force range measured, -0.5 to $+0.3$ g, the weighing device used had an accuracy of $\sim \pm 0.003$ g. Several attempts were made to ensure more reliable data on the jet shape than previously available.

The tube nozzles used were of 7.56, 8.10, and 17.1 mm ID and much larger than ordinary nozzles. Each nozzle was cut off sharply and conically at the exit end, as shown in Figure 1, in order to prevent the liquid from attaching to the horizontal end plane facing downward that would have existed if it had not been cut off. Thus the fluid extruded from a vertical nozzle was observed to separate from the solid wall at the position of $z = 0$ and $r = R$ over the whole flow range of the present experiments. The consistency between the data on $a(z)$ and the data on F_0 was checked, and only those data of $a(z)$ that satisfied the macroscopic momentum equation, Eq. 5, are reported here. This is a very important and rigorous check on the reliability of any jet shape whether it be empirical or theoretical. Unfortunately, many data on jet shapes previously reported do not satisfy the requirement of the integral invariant even far downstream from the nozzle exit.

The main part of the apparatus is similar to the conventional one used in the study of spinning (Weinberger and Goddard, 1974); it is shown in Figure 2. The liquid was supplied from a head tank to the tube nozzle to make a vertical jet through a long fixed tube. The flow rate was controlled with a valve attached to the tank bottom. The apparatus was installed at a position high enough that a series of photographs could be taken along a vertical jet of about 80 cm length. A damper to prevent vibration was attached to the device for force measurement. The vertical nozzle mainly used was a stainless steel tube of 7.65 mm dia., 10 cm long. The volumetric flow rate, the total axial force at a nozzle exit, and the jet shape were determined by experiments. The liquids used were glycerol-water solutions (GW), castor oils (CO), silicone oils (SO), and poly(oxyethylene · oxypropylene) glycol (PG). Their viscosity ranged from 5.58×10^{-3} to 77.8 Pa · s, and their surface tension changed between 0.022 and 0.068 N/m.

The consistency between the two kinds of experimental data on the axial force and the jet shape was checked by using the macroscopic momentum equation, Eq. 5, with Eqs. 8 and 9. Figure 3 shows the variations of the following three terms:

$$\mathrm{I} = F/\pi R^2 \rho \bar{u}_0^2$$

$$\mathrm{II} = W/\pi R^2 \rho \bar{u}_0^2$$

$$\mathrm{I} + \mathrm{II} \qquad (10)$$

The data were obtained from jet 3 with the flow conditions in Table 1. As z increases, the weight of the liquid filament W also increases, but the axial force F acting at the position z decreases due to the negative term of $-\rho \bar{u}^2$ in Eq. 9. Both variations on the righthand side of Eq. 5 cancel and their sum is kept constant along the z axis according to the requirement of the integral invariant. Moreover, the constant value calculated from the jet shape function $a(z)$ is almost equal to the measured value of F_0 ($= -0.94$) according to the macroscopic momentum equation, Eq. 5.

Results

F_0 and $\dot{a}_0$

As seen in Eq. 8, the total axial force exerted at the tube exit on a jet filament consists of the three terms of surface tension, force of inertia, and pressure. At a low flow rate the inertia term, $\rho \bar{u}_0^2$, is negligible and the jet filament is supported by the surface tension and the suction pressure, as in the case of a stationary drop. This negative pressure, $(p_0 - p_a)$, must increase linearly with increasing $\mu \bar{u}_0/d$, since the weight of the suspending jet filament increases owing to the viscous drag while the surface tension in the axial direction will change only a little. Such a

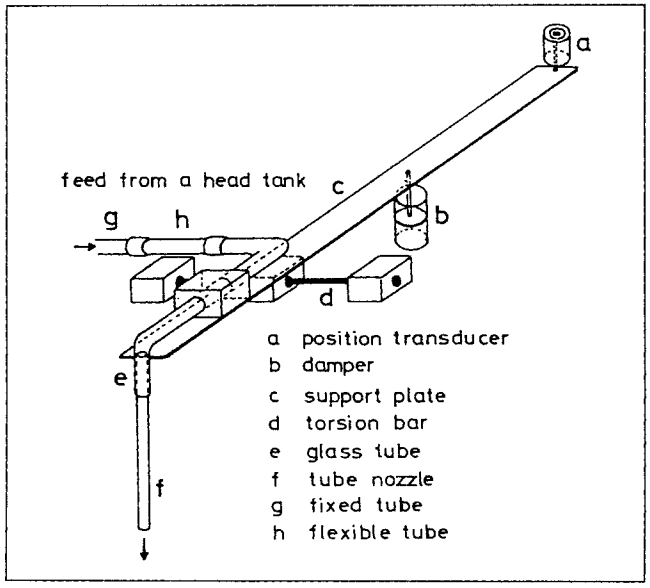

Figure 2. Force measuring device and vertical tube nozzle for a jet.

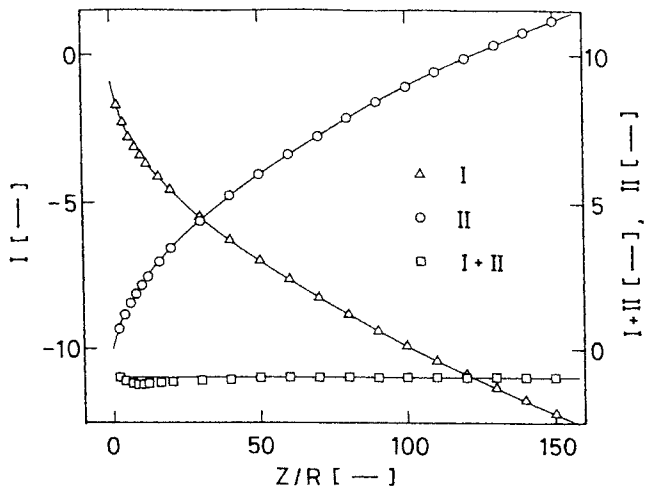

Figure 3. Estimation of exit axial force as an integral invariant from jet 3, Table 1.

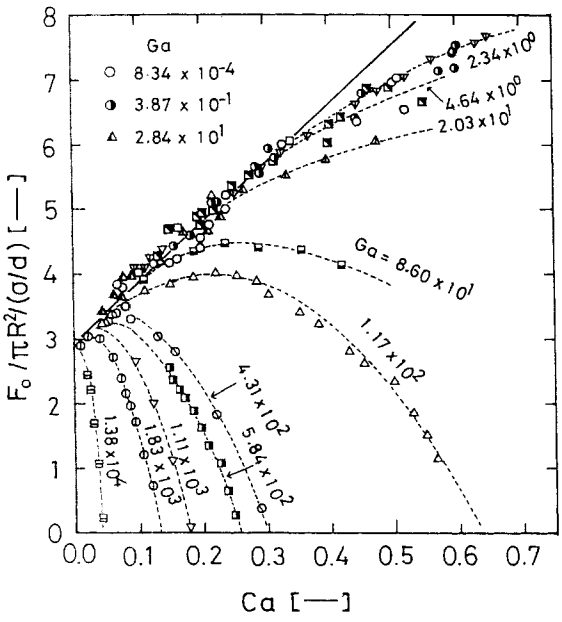

Figure 4. Experimental data of F_0 for vertical jets.

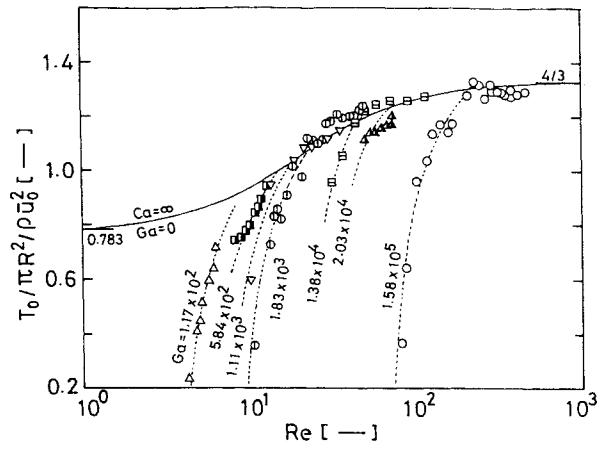

Figure 5. Effect of gravity on jet thrust.

physical situation is seen in Figure 4 as a straight solid line tangential to the experimental curves of F_0 at low flow rates. This straight line is expressed by

$$F_0/\pi R^2/(\sigma/d) = 9.2\,\mathrm{Ca} + 2.95 \tag{11}$$

It is reasonable that the constant value of 2.95 for $Ca \to 0$ is between the value of 3.5 reported by Hozawa et al. (1981) for the largest stationary drop hanging from a vertical tube and that of 2.6 given by Otake and Fujita (1949) for a drop falling in a quasistatic state. At a higher flow rate the effect of inertia becomes more important, and the experimental curves of F_0 start to deviate from the straight line of the viscous-gravity jet for which the gravitational force balances the viscous drag. As the flow rate increases, the increasing rate of F_0 owing to viscous drag is suppressed gradually by the effect of inertia, as anticipated from Eq. 8. F_0 reaches a maximum value, and then it begins to decrease. As the flow rate increases much more, F_0 changes its sign. This negative force is known as the jet thrust. As the Galileo number Ga decreases, experimental curves start to deviate and fall at a higher capillary number Ca; however, they do not seem to rise up to the straight line in a region of $Ca >$ 0.4 however low Ga may be.

For an inertia-gravity jet, the inertia force balances the gravitational force and we can expect that $F_0 \propto -p\bar{u}_0^2$, although the effect of surface tension is not negligible at a low flow rate. The experimental data of F_0 for $Ga > 10^4$ were almost represented by a single line of

$$\frac{F_0}{\pi R^2 \rho g d} = -1.31\,Fr + 0.370 \tag{12}$$

although such a figure is not presented here. The slope corresponds reasonably to $-4/3$, the value obtained from Harmon's (1955) prediction, and the constant value of 0.370 extrapolated to the zero flow rate is mainly due to the surface tension.

When the flow is dominated by the inertia, the jet thrust T_0 defined by Eq. A4 is often used in place of the exit axial force F_0. Substituting Eq. A4 into Eq. 8, we obtain

$$T_0 = 2\pi R\sigma/\sqrt{1 + \dot{a}_0^2} - F_0 \tag{13}$$

where $\dot{a}_0$ and F_0 are determined by the present experiments. The results of T_0 are shown in Figure 5. The solid line is the same one as given in Figure 12 for the case of neither gravity nor surface tension. The present experimental data show that the gravitational force produces a decrease in the jet thrust because the negative exit pressure caused by the hanging effect of a jet filament becomes significant with an increasing effect of gravity. However, as the flow rate increases, the effect of inertia becomes more significant and all the experimental curves approach the solid line.

The initial slope of shape curve $\dot{a}(0)$ is indispensable for estimation of the surface tension term in Eq. 13 and also useful as one of the boundary conditions to an ordinary differential equation for the one-dimensional model of a free falling jet. The experimental data are shown in Figure 6. Each curve represents the data for a liquid and a tube nozzle. The computational results of Omodei (1980) for a gravity-free case are also given in the figure. As the flow rates increase, the experimental curves seem to approach asymptotically the curves of the gravity-free case. As the flow rates decrease, the curves become almost parallel lines with the same constant slope.

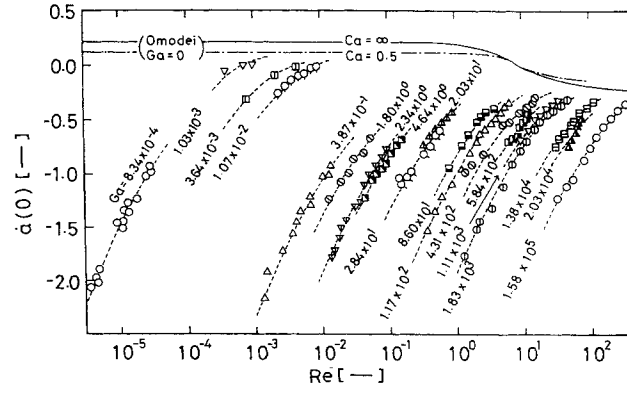

Figure 6. Experimental data of $\dot{a}(0)$ for vertical jets.

Table 1. Flow Conditions and Axial Forces for Jets Presented in Figure 7

Jet No.	Re	Fr	We	N_j	$(ReFr)^{1/2}$	$F_0/\pi R^2\rho\bar{u}_0^2$	Liquids*
1	4.97×10^2	1.57×10^0	1.56×10^1	3.16×10^2	2.79×10^1	-1.06	GW 0.06
2	3.96×10^2	9.92×10^{-1}	9.88×10^0	3.99×10^2	1.98×10^1	-0.92	GW 0.06
3	1.17×10^2	1.00×10^0	1.01×10^1	1.17×10^2	1.08×10^1	-0.94	GW 0.2
4	5.52×10^1	1.67×10^0	1.90×10^1	3.31×10^1	9.61×10^0	-1.02	GW 0.6
5	4.67×10^1	1.19×10^0	1.36×10^1	3.92×10^1	7.45×10^0	-0.99	GW 0.6
6	3.70×10^1	8.43×10^{-1}	8.18×10^0	4.39×10^1	5.59×10^0	-0.67	GW 0.6
7	1.68×10^1	6.16×10^{-1}	6.39×10^0	2.73×10^1	3.22×10^0	-0.70	GW 1.2
8	6.27×10^0	3.29×10^{-1}	3.55×10^0	1.91×10^1	1.44×10^0	$+0.325$	GW 2.4
10	8.97×10^0	1.75×10^{-1}	1.81×10^0	5.13×10^1	1.25×10^0	$+1.10$	GW 1.2
12	3.98×10^0	1.58×10^{-1}	1.67×10^0	2.52×10^1	7.93×10^{-1}	$+2.00$	GW 3
13	2.27×10^0	4.98×10^{-2}	5.26×10^{-1}	4.56×10^1	3.36×10^{-1}	$+9.2$	GW 3
14	9.58×10^{-1}	3.87×10^{-2}	4.12×10^{-1}	2.48×10^1	1.93×10^{-1}	$+1.50 \times 10^1$	GW 6
15	4.12×10^{-1}	7.18×10^{-3}	7.65×10^{-2}	5.74×10^1	5.44×10^{-2}	$+6.30 \times 10^1$	GW 6
16	1.45×10^{-1}	4.46×10^{-3}	4.82×10^{-2}	3.25×10^1	2.54×10^{-2}	$+1.17 \times 10^2$	GW 12
19	7.97×10^{-2}	2.57×10^{-3}	3.86×10^{-2}	3.10×10^1	1.43×10^{-2}	$+1.76 \times 10^2$	CO 13
22	7.39×10^{-2}	1.91×10^{-3}	2.06×10^{-2}	3.76×10^1	1.17×10^{-2}	$+2.70 \times 10^2$	GW 16
24	6.50×10^{-2}	8.72×10^{-4}	9.41×10^{-3}	7.45×10^1	7.53×10^{-3}	$+4.75 \times 10^2$	GW 12
25[a]	4.39×10^{-3}	5.29×10^{-3}	1.13×10^{-1}	8.30×10^{-1}	4.82×10^{-3}	$+5.3 \times 10^2$**	SO 300
26[b]	6.33×10^{-3}	3.76×10^{-3}	2.91×10^{-1}	1.68×10^0	4.87×10^{-3}	$+5.4 \times 10^2$**	PG 800
27	4.05×10^{-2}	5.74×10^{-4}	6.20×10^{-3}	7.06×10^1	4.82×10^{-3}	$+7.47 \times 10^2$	GW 16
28[b]	4.72×10^{-3}	2.09×10^{-3}	1.62×10^{-1}	2.26×10^0	3.14×10^{-3}	$+8.5 \times 10^2$**	PG 800
30[a]	2.08×10^{-3}	1.19×10^{-3}	2.98×10^{-2}	1.75×10^0	1.57×10^{-3}	$+1.67 \times 10^3$**	SO 300
32[c]	9.57×10^{-4}	8.92×10^{-4}	1.54×10^{-2}	1.07×10^0	9.23×10^{-4}	$+3.1 \times 10^3$**	PG 800
34[c]	6.98×10^{-4}	4.75×10^{-4}	8.18×10^{-3}	1.47×10^0	5.76×10^{-4}	$+4.9 \times 10^3$**	PG 800
35[a]	7.73×10^{-4}	1.64×10^{-4}	4.11×10^{-3}	4.71×10^0	3.56×10^{-4}	$+7.4 \times 10^3$**	SO 300
36[c]	3.75×10^{-4}	1.19×10^{-4}	2.06×10^{-3}	3.15×10^0	2.11×10^{-4}	$+1.3 \times 10^4$**	PG 800

*GW, glycerol-water; CO, castor oils; SO, silicone oils; PG, poly(oxyethylene · oxypropylene) glycol
**F_0 calculated
a. Nozzle of $d = 0.810$ cm, $l = 0.860$ cm
b. Nozzle of $d = 1.71$ cm, $l = 2.14$ cm
c. Nozzle of $d = 0.805$ cm, $l = 2.08$ cm

a(z) results

The flow conditions for experimental results of the jet shape are given in Table 1. The jet numbers in the first column correspond to the order of the shape curves presented in Figure 7 although some have been omitted in the figure. The order is not explained by any single dimensionless number, Re, Fr, or N_j, but it can almost be correlated by $Re \cdot Fr$. The importance of this parameter is seen also in Eqs. 2 and 3 of Clarke (1968). Shape curves for lower speed jets are located on the right side and those for higher speed jets are located on the left side in Figure 7. As shown, any jet shape curve approaches asymptotically a single solid line downstream as the inertia force grows to balance the gravitational force. This line is of the inertia-gravity jet expressed by the Scriven-Pigford equation, Eq. 2 with $\delta_i = 1$. The experimental data of jets 1–6 were also represented well by the same solid line over the whole jet length corresponding to the flow conditions of $\rho g d \simeq \rho\bar{u}_0^2 \gg \rho\bar{u}_0/d$. On the other hand, the experimental data of jets 28–36 were represented except at the tails of falling jets by a single line in the $a/R - \sqrt{N_j}\, z/R$ correlation chart (the chart is not shown here). This line is of the viscous-gravity jet described by

$$(N_j/24)^{1/2}\, z/R = R/a - 1 \qquad (14)$$

which is valid for the flow conditions of $\rho g d \simeq \mu\bar{u}_0/d \gg \rho\bar{u}_0^2$.

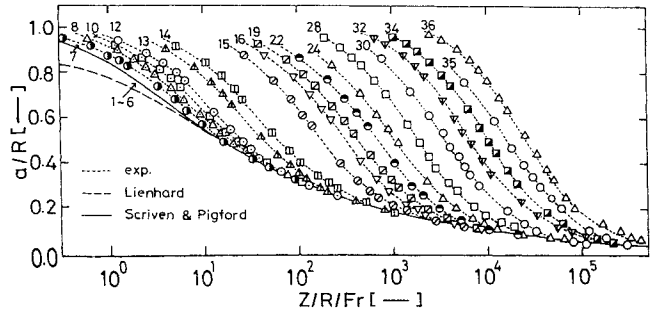

Figure 7. Experimental data of $a(z)$ for vertical jets.

Validity of Eq. 4

For $Re \simeq N_j \simeq 0(10^2)$, experimental data of jet 2 are compared with curves 1, 4, and 5 in Figure 8, and for $Re \simeq N_j \simeq 0(10)$, experimental data of jet 5 are compared with curves 1, 2, and 3. The predictions of Eq. 4 are good in the region of $z/R > 1$ for the first case and in the region of $z/R > 8$ for the second case. However, the prediction of Scriven and Pigford (1959), curve 1, is best in a range of $Re \simeq N_j > 0(10)$. Experimental work of Kurabayashi (1959) and Mendizabal et al. (1987) also supported Eq. 1 with $\delta_i = 1$. Therefore, Eq. 4 will give a better prediction if we use $\delta_i = 1$ in the relevant range of flow conditions.

Figure 9 shows that the predictions of Eq. 4 with $\delta_i = 0.613$

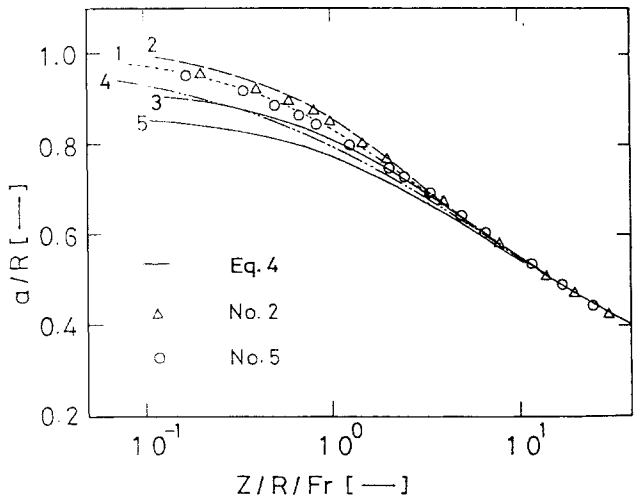

Figure 8. Predicted and measured jet shapes for $Re > 0$ (10).

1. Scriven-Pigford
2. Shirazi ($Re = N_j = 50, Fr = 1, We = \infty$)
3. Eq. 4 ($Re = 50, Fr = 1, We = \infty$)
4. Duda-Vrentas ($Re = Fr = \infty, N_j = 128.6, We = 5.4$)
5. Eq. 4 ($Re = We = \infty$)

and $\delta_v = 1/1.13$ agree well with the computational results of Shirazi (1978) at $Re = 1$. In a wide range of $Re = 0(1) \sim 0(10^{-3})$, reasonable agreements between predictions of Eq. 4 and the present experimental data of jets 12, 15, 24, and 30 are shown in Figure 10.

In a range of creeping flow, the validity of Eq. 4 is tested in Figure 11 in comparison with the experimental data of Trang and Yeow (1976) for $N_j = 0.117$ and 0.503 as well as with the present experimental data of jets 32 and 36 for $N_j = 1.07$ and 3.15. A small disagreement with Trang and Yeow's data is seen in the upper portion of a jet. However, we can eliminate this disagreement if we change the value of a_{max}/R from 1.13 to a measured value, 1.05 or 1.02. Moreover, we would obtain much modified agreement over the whole range of jet length if we could take account of the effect of inertia at the tail of a jet.

Thus we have found that Eq. 4 is useful over a wide range of flow conditions. However, its predictions will be much modified if we can take proper values for the two adjustable parameters, δ_i and δ_v, by taking account of experimental and computational results.

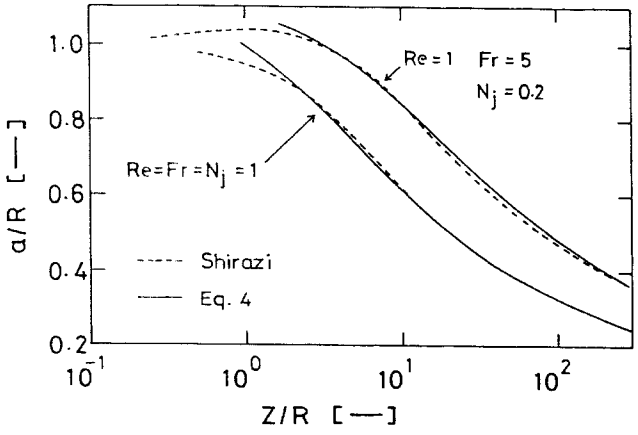

Figure 9. Predictions of Eq. 4 and computational results of Shirazi (1978) at $Re = 1$.

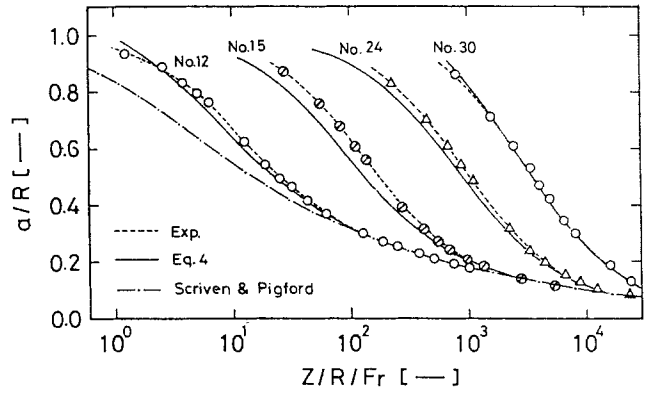

Figure 10. Predicted and measured jet shapes for $Re = 0$ (1) ~ 0 (10^{-3}).

Conclusions

The shape function of a laminar, liquid jet emerging from a round vertical tube into the atmosphere and the total force exerted on the liquid filament at the tube exit was investigated by experiments:

1. Experimental data of $a(z)$, $\dot{a}_0$, and F_0 have been presented for a wide range of flow conditions under a significant effect of gravity.
2. The experimental data of F_0 and $a(z)$ for the two extreme flow conditions of a viscous-gravity jet and a inertia-gravity jet have been expressed by analytical equations.
3. Equation 4 to predict $a(z)$ is useful over a wide range of flow conditions.

Acknowledgment

The authors wish to thank Dr. Nakamura of Kyoto University for his kind advice in making the force measurement device. The authors are also grateful to Dr. MacSporran of the University of Bradford for bringing the cited work of Anno and Shirazi to their attention.

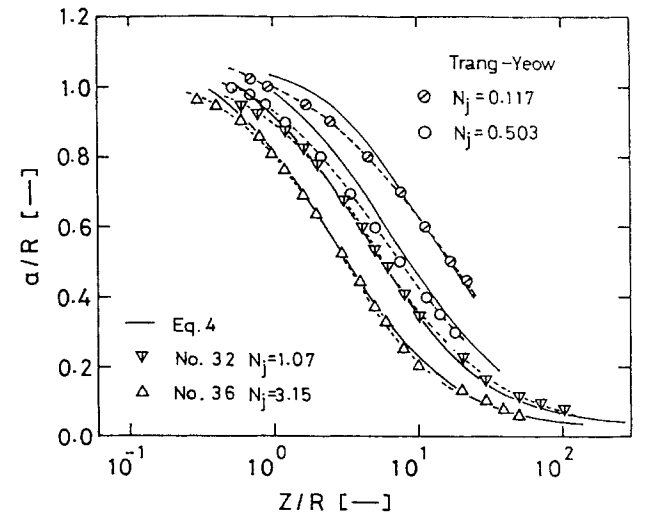

Figure 11. Predicted and measured shapes of a creeping jet.

Notation

A_i = Airy function
$a, \dot{a}$ = jet radius and da/dz
a_x, a_{max} = maximum jet radius of horizontal, vertical jet
Bo = bond number, $d^2\rho g/\sigma$
Ca = capillary number, $\mu\bar{u}_0/\sigma$
d = inner diameter of a nozzle tube, $2R$
F = total axial force exerted on a filament
Fr = Froude number, $\bar{u}_0^2/dg$
Ga = Galileo number, $d^3\rho\pi^2/\mu^2$
g = gravitational acceleration
k = adjustable parameter, Eq. 2
l = nozzle length
N_j = Stokes number, $d^2g\rho/\bar{u}_0\mu$
p, p_a = hydrodynamic, ambient pressure
R = inner radius of nozzle tube
Re = Reynolds number, $d\bar{u}_0\rho/\mu$
r = radial coordinate
T = jet thrust
u = axial velocity component
W = weight of a suspending filament
We = Weber number, $d\bar{u}_0^2\rho/\sigma$
z = axial coordinate
I, II = defined in Eq. 10

Greek letters

δ_i, δ_v = adjustable parameters, Eq. 4
μ = liquid viscosity
ρ = liquid density
σ = liquid surface tension
τ_{zz}, τ_w = deviatoric axial stress, wall shear stress

Subscripts

0 = value at nozzle exit ($z = 0$)

Superscripts

$-$ = value averaged over the horizontal cross section

Literature Cited

Adachi, K., "Laminar Jets of a Plane Liquid Sheet Falling Vertically in the Atmosphere," *J. Non-Newt. Fluid Mech.*, **24,** 11 (1987).

Adachi, K., and N. Yoshioka, "Tube Exit Flows and Laminar Newtonian Jets in the Atmosphere," *Advances in Rheology,* B. Mena, A. Garcia-Rejon, C. Rangel-Najaile, eds., Universidad Nacional Autonoma de Mexico, **2,** 239 (1984).

Adachi, K., T. Aoki, S. Nishida, and R. Nakamura, "A Hydrodynamic Investigation of a Falling Liquid Film for Curtain Coating and Sheet Casting," *Proc. 10th Int. Cong. Rheology,* **1,** 122 (1988).

Anno, J. N., *The Mechanics of Liquid Jets,* Lexington Books, Heath, Lexington, MA (1977).

Clarke, N. S., "Two-Dimensional Flow under Gravity in a Jet of Viscous Liquid," *J. Fluid Mech.*, **31,** 481 (1968).

Cruickshank, J. O., "A Similarity between Plane and Axisymmetric Viscous-Gravity Jets," *Trans. ASME J. Fluids Eng.*, **106,** 52 (1984).

Davies, J. M., J. F. Hutton, and K. Walters, "A Critical Reappraisal on the Jet Thrust Technique for Normal Stresses, with Particular Reference to Axial Velocity and Stress Rearrangement at the Exit Plane," *J. Non-Newt. Fluid Mech.*, **3,** 141 (1977/1978).

Duda, J. L., and J. S. Vrentas, "Fluid Mechanics of Laminar Liquids Jets," *Chem. Eng. Sci.*, **22,** 855 (1967).

Dutta, A., and M. E. Ryan, "Dynamics of a Creeping Newtonian Jet with Gravity and Surface Tension: A Finite-Difference Technique for Solving Steady Free-Surface Flows Using Orthogonal Curvilinear Coordinates," *AIChE J.*, **28,** 220 (1982).

Georgiou, G. C., T. C. Papanastasiou, and J. O. Wilkes, "Laminar Newtonian Jets at High Reynolds Number and High Surface Tension," *AIChE J.*, **34,** 1559 (1988).

Goren, S. L., and S. Wronski, "The Shape of Low Speed Capillary Jets of Newtonian Liquids," *J. Fluid Mech.*, **25,** 185 (1966).

Harmon, D. B., "Drop Sizes from Low Speed Jets," *J. Franklin Inst.*, **259,** 519 (1955).

Hozawa, M., T. Tsukada, N. Imaishi, and K. Fujinawa, "Effect of Wettability on Static Drop Formation from a Hole in Horizontal Flat Plate," *J. Chem. Eng. Japan,* **14,** 358 (1981).

Joseph, D. D., "An Integral Invariant for Jets of Liquid into Airs," *Arch. Rational Mech. Anal.*, **74,** 389 (1980).

Joseph, D. D., K. Nguyen, and J. E. Matta, "Jets into Liquid under Gravity," *J. Fluid Mech.*, **128,** 443 (1983).

Kurabayashi, T., "Atomization of Liquids by Means of a Rotating Nozzle," *Trans. Japan Soc. Mech. Eng.*, **25,** 185 (1959).

Lienhard, J. H., "Effects of Gravity and Surface Tension upon Liquid Jets Leaving Poiseuille Tubes," *Trans. ASME J. Basic Eng.*, **90,** 262 (1968).

Mendizabal, D. G., C. O. Fuentes, and J. M. Guzman, "Hydrodynamics of Laminar Liquid Jets. Experimental Study and Comparison with Two Models," *Chem. Eng. Comm.*, **56,** 117 (1987).

Middleman, S., and J. Gavis, "Expansion and Contraction of Capillary Jets of Newtonian Liquids," *Phys. Fluids,* **4,** 355 (1961).

Nickell, R. E., R. I. Tanner, and B. Caswell, "The Solution of Viscous Incompressible Jet and Free Surface Flows Using Finite-Element Methods," *J. Fluid Mech.*, **65,** 189 (1974).

Oliver, D. R., and R. C. Ashton, "The Flow of Polymer-Thickened Oils in Convergent Jet-Thrust Nozzles at a Temperature of 84°C," *J. Non-Newt. Fluid Mech.*, **4,** 345 (1979).

Omodei, B. J., "On the Die-Swell of an Axisymmetric Newtonian Jet," *Comput. Fluids,* **8,** 275 (1980).

Otake, T., and S. Fujita, "On the Size of a Drop Formed at the Tube End," *Kagaku Kikai* (Japan), **13,** 199 (1949).

Petrie, C. J. S., *Elongational Flows,* Pitman, London (1979).

Scriven, L. E., and R. L. Pigford, "Fluid Dynamics and Diffusion Calculations for Laminar Liquid Jets," *AIChE J.*, **5,** 397 (1959).

Shirazi, A. F., "Fluid Mechanics of Horizontal and Vertical Laminar Newtonian Jets," Ph. D. Thesis, Illinois Inst. Technol. (1978).

Trang, C. T., and Y. L. Yeow, "Extrudate Swell of Newtonian and Non-Newtonian Fluids—The Effect of Gravitational Body Force," *J. Non-Newt. Fluid Mech.*, **20,** 103 (1986).

Trouton, F. T., "On the Coefficient of Viscous Traction and Its Relation to that Viscosity," *Proc. Roy. Soc.*, **A77,** 426 (1906).

Weinberger, C. B., and J. D. Goddard, "Extensional Flow Behavior of Polymer Solutions and Particle Suspensions in a Spinning Motion," *Int. J. Multiphase Flow,* **1,** 465 (1974).

Appendix

Substituting Eqs. 7 and 9 into 5 and differentiating the result with z, we have an ordinary differential equation for a one-dimensional jet flow model. That equation gives the following two limiting solutions:

For $Re \simeq 0$

$$\frac{z}{R} = \left\{\frac{2}{Bo} + \left[\left(\frac{2}{Bo}\right)^2 + \frac{24}{N_j}\right]^{1/2}\right\}\left(\frac{z}{a} - \delta_v\right) \tag{A1}$$

For $Re \gg 1$

$$\frac{1}{Fr}\frac{z}{R} = \left(\frac{R}{a}\right)^4 - \delta_i \tag{A2}$$

It should be remarked that Eq. A1 is always invalid sufficiently far downstream, because even at a very low Reynolds number the inertia force will eventually grow so that it overwhelms the viscous force and balances the gravitational force. Thus the tail of any vertical jet will be expressed by Eq. A2.

For a creeping jet, it is not unreasonable to put $\delta_v = 1$ in Eq. A1 because the velocity profile $u(r)$ becomes almost flat within the distance of one nozzle diameter, $2R$, downstream from the nozzle exit. When the jet swells, however, $\delta_v = R/a_{max}$ and the origin of z is set at the position of the maximum jet diameter.

The swelling ratio of a vertical jet is still unknown, so that of a horizontal jet is used. Thus, $\delta_v = 1$ for $Re \geq 14$, and $\delta_v = \delta_i^{1/4}$ for $Re < 14$.

For an inviscid fluid, the velocity profile at the nozzle exit is flat, so that $\delta_i = 1$ in Eq. A2. For a high-speed jet of a viscous liquid, the velocity profile is almost parabolic, and there is a long transient zone between the nozzle exit and the zone of flat velocity profile. A proper choice of the constant value δ_i is effective for validity of Eq. A2, especially in this transient zone.

We use the macroscopic momentum equation to determine a proper value for δ_i. Substituting $u(z)$ derived from Eq. A2 into the righthand side of Eq. 5 and estimating the result at a distance far downstream from the nozzle, we have a constant, $-\delta_i^{1/2}$ for $(F + W)/\pi R^2 \rho \bar{u}_0^2$. Taking into account that the inertia force is superior to the surface tension and the gravitational force at the nozzle exit for a highspeed jet, we obtain from Eq. 5

$$\delta_i = (T_0/\pi R^2 \rho \bar{u}_0^2)^2 \tag{A3}$$

where T_0 is called jet thrust and defined by

$$T_0 = 2\pi \int_0^R (p_0 - p_a + \rho \bar{u}_0^2) r \, dr \tag{A4}$$

The jet thrust for a high-speed, vertical jet is considered almost equal to that for a horizontal jet, so we can evaluate T_0 through previous computational and experimental results on jet shapes (Middleman and Gavis, 1961; Goren and Wronski, 1966; Nickell et al., 1974; Shirazi, 1978; Omodei, 1980). All these results of T_0 have been plotted in Figure 12 with experimental data of jet thrusts (Davies et al., 1978; Oliver and Ashton, 1979). All the data are almost represented by a single solid curve, as shown previously by Davies et al. (1978). This curve is expected to approach 4/3 with increasing Re in accordance with Harmon's (1955) prediction and also to go asymptotically to 0.783 with decreasing Re, in agreement with the accepted value of die swell ($a_\infty/R = 1.13$).

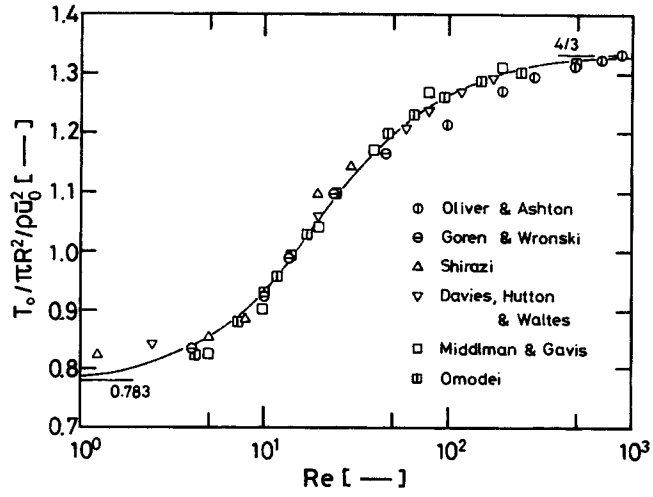

Figure 12

As Re decreases, the effects of gravitational force and surface tension become significant. Then the value of δ_i obtained in the above way is inaccurate. In such a case, however, the inaccuracy of δ_i in Eq. 4 is veiled to some extent by the existence of the last term for a low-speed jet.

Manuscript received July 5, 1988, and revision received Sept. 8, 1989.